의학박사 학위논문

Studies on the role of phosphorylation of alpha-synuclein in alpha-synuclein degradation pathway

: Phosphorylation of Y136 is crucial in compensating for proteasomal dysfunction.

알파 시누클레인 분해 경로에 있어서 알파 시누클레인의 인산화의 역할에 관한 연구

2013 년 8 월

서울대학교 대학원

의과대학 의학과 약리학 전공

최 희 순

Studies on the role of phosphorylation of alpha-synuclein in alpha-synuclein degradation pathway

: Phosphorylation of Y136 is crucial in compensating for proteasomal dysfunction.

지도교수 김 용 식

이 논문을 의학박사 학위논문으로 제출함

2013 년 8 월

서울대학교 대학원

의과대학 의학과 약리학 전공

최 희 순

최희순의 의학박사 학위논문을 인준함

2013 년 8 월

위 원 장 나 종 이 (인)

부위원장 김 용 식 (인)

위 원 조 맹 제 (인)

위 원 김 혜 선 (인)

위 원 황 은 유 (인)

Studies on the role of phosphorylation of alpha-synuclein in alpha-synuclein degradation pathway

: Phosphorylation of Y136 is crucial in compensating for proteasomal dysfunction.

By

Hee Soon Choi

A thesis submitted to the Department of Pharmacology in partial fulfillment of the requirements for the Degree of Doctor of Philosophy in Pharmacology at the Seoul National University College of Medicine

August, 2013

Approved by thesis committee

Professor _____ Chairman

Professor _____ Vice Chairman

Professor _____

Professor _____

Professor _____

ABSTRACT

Studies on the role of phosphorylation of alpha-synuclein in alpha-synuclein degradation pathway

: Phosphorylation of Y136 is crucial in compensating for proteasomal dysfunction.

Hee Soon Choi

Department of Pharmacology, College of Medicine

The Graduate School

Seoul National University

α-Synuclein (α-SYN) has been characterized as a heat-stable and aggregation-prone protein that can be degraded by both the ubiquitin-proteasomal pathway and the chaperone-lysosomal pathway. However, the switching mechanism between the two pathways is not well understood. In my study, I investigated the increase of the binding of α-SYN to heat shock protein 70 cognate (HSC70) and the lysosomal translocation of α-SYN. Tyrosine phosphorylation at Y136 of α-SYN increased its binding to HSC70. I also found that Y136 phosphorylation of α-SYN can be regulated by the focal adhesion kinase pp125 (FAK) and protein tyrosine phosphatase 1B (PTP1B). Furthermore, a PTP1B inhibitor prevented the accumulation of α-SYN in SH-SY5Y cells by increasing α-SYN translocation into the lysosome, protected dopaminergic neurons against cell death and rescued

Rotarod performance in a Parkinson's disease (PD) model. I provide evidence that the regulation of the phosphorylation of α-SYN at Y136 can improve behavioral performance and protect dopaminergic neurons against cell death through enhanced lysosomal degradation of α-SYN.

Keywords: α-synuclein, proteasome, lysosome, tyrosine, Parkinson's disease, phosphorylation

Student Number: 2006-30572

CONTENTS

LIST OF FIGURES

LIST OF ABBREVIATIONS

HSC70, Heat shock protein 70 cognate

FAK, Focal adhesion kinase

PTP1B, Protein tyrosine phosphatase 1B

PD, Parkinson's disease

α-SYN, Alpha synuclein

UPS, Ubiquitin proteasome system

CMA, Chaperone mediated autophagy

Ub, Ubiquitin

GAPDH, Glyceraldehyde 3-phosphate dehydrogenase

FBS, Fetal bovine serum

DMEM, Dulbercco's modified Eagle's medium

BSA, Bovine serum albumin

NGS, Normal goat serum

IPTP, Isopropyl β-D-1-thiogalactopyranoside

GST, Glutathione S-transferase

I.P., Intraperitoneal

PQ, Paraquat

TH, Tyrosine hydroxylase

CK1, Casein kinase1

CK2, Casein kinase2

PTKs, Protein tyrosine kinases

INTRODUCTION

Parkinson's disease (PD) is caused by the progressive degeneration and loss of dopaminergic neurons and is characterized by α-synuclein containing cytoplasmic inclusions known as Lewy bodies in the Substantia nigra (1, 2).

α-SYN exists in presynaptic nerve terminals and is an intrinsically unfolded acidic neuronal protein composed of 140 amino acids (3). α-SYN can be normally degraded by the ubiquitin-proteasomal pathway and the autophagy-lysosomal pathway. A number of studies have verified that both of these pathways are relevant to the clearance of α-SYN (4-7). Specifically, aggregates of α-SYN are removed by passing through the autophagy-lysosomal pathway (5).

Recently, the importance of the ubiquitin-proteasomal pathway has been highlighted in neurons and many researchers have become interested in understanding the role of proteolytic systems in neurodegenerative diseases. Because neuronal intracellular inclusions consist of ubiquitin-attractive protein aggregates that are thought to be a common characteristic of several neurodegenerative diseases, such as Parkinson's disease (PD) (8-10), Alzheimer's disease(AD) (11-13), Huntington's disease (HD) (14-16), amyotrophic lateral sclerosis (ALS) (17, 18), and prion diseases (19), it has been hypothesized that the failure of the ubiquitin proteasome system (UPS) is the etiological cause of many neurodegenerative diseases (20).

An impairment of the function of the ubiquitin-proteasomal pathway or the autophagy-lysosomal pathway results in the accumulation of α-SYN aggregates, which have the cellular toxicity (7). α-SYN can pass through the macroautophagy (21) and chaperone-mediated autophagy (CMA) pathways (6, 22) (23).

The characteristic feature of macroautophagy is the formation of double membrane cytosolic vesicles known as autophagosomes by the sequestration of cargo. After fusion of the autophagosome with lysosomes, α-SYN is degraded in the autophagolysosome (24, 25). CMA involves the selective targeting of specific cytosolic proteins as well as α-SYN to the lysosome. The target substrate proteins, which contain a KFERQ-related peptide motif, are translocated to the lysosome through the interaction with a lysosomal chaperone, HSC70 and a lysosomal receptor, lysosomal associated membrane protein 2A (LAMP-2A) (26, 27). α-SYN contains a CMA recognition motif $_{95}$-VKKDQ-$_{99}$ (28, 29) and binds to HSC70 through this motif for degradation by CMA (29).

Autophagy is a degradation pathway for cytosolic components via the lysosome, and the targets of autophagy are misfolded proteins, long-lived, stable proteins, protein aggregates and even cellular organelles. Because the large size of membrane proteins or protein complexes cannot pass through the proteasome, these components can be degraded by autophagy (6, 30-32). As the part of the protein quality control system, autophagy, in common with the ubiquitin-proteasomal pathway, plays a direct role in protein conformational disorders and

neurodegeneration. The impairment of autophagic degradation of α-SYN works as an important mechanism causing neurodegeneration (6, 33, 34). Unlike the ubiquitin-proteasomal pathway, autophagy can degrade a very broad range of target components. If the factors and mechanisms related to α-SYN degradation pathway, ubiquitin-proteasomal or autophagy-lysosomal pathway, are known, one can understand the pathogenic mechanisms of PD.

The post-translational modifications of α-SYN include phosphorylation (35, 36), oxidation (37), nitration (38, 39), sumoylation (40), and ubiquitination (41, 42). Some studies have shown that α-SYN is phosphorylated at serine residues (Ser87, Ser129) and tyrosine residues (Tyr125, Tyr133, Tyr136) (43, 44), and other studies have suggested that phosphorylation of these residues is related to changes in α-SYN location (45). In addition, functional regulation by phosphorylation has been reported: tyrosine phosphorylation of α-SYN at residue 125 inhibits toxic oligomer formation and protects neurons from neurotoxicity in *Drosophila* PD model, while serine phosphorylation has oligomer-promoting effects (46).

In this study, I demonstrated that the induction and maintenance of phosphorylation of α-SYN tyrosine residues, especially Y136, can accelerate α-SYN degradation. I also confirmed that activation of the autophagy-lysosomal pathway was induced under the same condition. Furthermore, the increase of autophagic lysosmal function in neurodegenerative disease models enhanced the

degradation of misfolded or aggregated α-SYN and reduced cellular toxicity. In the case of α-SYN, the crucial factor for survival of the neuronal cells is the rapid induction of α-SYN degradation pathways, which can be activated by changes in the condition of the cells or the environment around the cells. Because each protein interacted with α-SYN is different in the two degradation pathways as ubiquitin and chaperone, the mechanisms for inducing their interactions with α-SYN have attracted attention. The modification process, mechanisms and molecules involved in determining α-SYN degradation pathway are not yet fully understood. Accordingly, understanding the regulation of α-SYN degradation in neuronal cells can facilitate development of therapeutic drugs for PD.

MATERIALS AND METHODS

Ethics statement

The animals used in this experiment were handled according to the Guidelines for Animal Experimentation. This study was approved by the Ethics Committee of Seoul National University Institutional Animal Care and Use (SNU IACUC; approval ID; SNU-110105-4).

Materials

DMEM and FBS for cell culture were purchased from Thermo Scientific (IL, USA). MG132, PTP1B inhibitor (3-(3,5-Dibromo-4-hydroxy-benzoyl)-2-ethyl-benzofuran-6-sulfonic acid-(4-(thiazol-2-ylsulfamyl-phinyl)- amide inhibitor) were purchased from Calbiochem (CA, USA), and 1,1'-Dimethyl-4-4'-bipyridinium dichloride hydrate (paraquat, PQ) was purchased from Sigma Aldrich (MO, USA). To silence the gene encoding FAK, siRNA was purchased from Santa Cruz Biotechnology (CA, USA). For immunoprecipitation and detection of tyrosine phosphorylated α-SYN, anti-α-SYN (211), anti-pY20, anti-HSC70, anti-Ub, anti- FAK, anti-p-FAK (925), anti-GAPDH antibodies, all of the HRP–conjugated antibodies and Western Blotting Luminol Reagent were purchased from Santa Cruz Biotechnology (CA, USA). Alexa Fluor 488 goat-anti-mouse IgG and LysoTracker® were purchased from Invitrogen (CA, USA).

Mouse anti-α-SYN and anti-LAMP1 (lysosomal-associated membrane protein 1) antibodies were purchased from BD Transduction Laboratories (KY, USA). The lysosome isolation kit was purchased from Sigma Aldrich (MO, USA) and the ubiquitination kit was purchased from Biomol International (PA, USA).

Immunoprecipitation and western blot

SH-SY5Y human neuroblastoma cells purchased from ATCC (American Type Culture Collection, VA, USA) were cultured with DMEM containing 10% FBS and antibiotics. For immunoprecipitaiton, cells were lysed with lysis buffer containing 50 mM Tris-Cl pH7.5, 150 mM NaCl, 25 mM β-glycerol phosphate, 1 mM EDTA, 1 mM EGTA, 10 mM NaF, 10 mM $MgCl_2$, 1% Nonidet P-40 and 0.3 mM Na_3VO_4 with protease inhibitor cocktail.

Protein G-agarose beads (Milipore, MA, USA) with cell lysate containing 1 μg of suitable antibody were rotated for 2 h at 4℃. After sedimentation by centrifuge at 5,000 rpm for 30 sec, the supernatants were discarded and the beads were washed with lysis buffer and boiled for 5min at 100℃. The boiled samples were separated by 12% SDS-PAGE and transferred onto nitrocellulose membrane. After blocking with 5% skim milk in phosphate-buffered saline containing 0.1% Tween20 (PBS-T), the membrane was immunoblotted with an appropriate antibody and developed using the western blotting Luminol reagent.

Immunocytochemistry and immunohistochemistry

For immunocytochemistry, after the media were discarded, the cells were stained with Lysotracker in DMEM for 30 min at 37 ℃. The cells were fixed with 4% paraformaldehyde, washed three times with PBS and blocked with blocking buffer containing 2% FBS, 2% BSA, 4% NGS and 0.2% Triton-X100. The cells were incubated with suitable primary antibody and an Alexa Fluor 488 tagged secondary antibody. After DAPI counter staining, the samples were mounted.

For immunohistochemistry, the brain was removed and fixed with 4% paraformaldehyde for 48 h at 4℃ and was embedded in paraffin. After the brain tissue slices attached to slides were incubated in the oven to melt the paraffin, the slides were deparaffinized and rehydrated by passing them through xylene, 100% ethanol, 95% ethanol, 80% ethanol, 70% ethanol and distilled water. For immunostaining, the slides were incubated with a suitable primary antibody overnight at 4℃ and rinsed three times with PBS. After the slides were incubated with Alexa 546-tagged secondary antibody for 1 h at room temperature and rinsed three times with PBS, the slides were mounted.

Each slide was observed by confocal microscopy.

In vitro ubiquitination assay

For the assay, ubiquitin, Mg-ATP, E1, E2 enzymes such as UBCH5a, UBCH5b, and UBCH8, SH-SY5Y cell lysate for the E3 ligase and histidine-tagged recombinant α-SYN were mixed gently and incubated at 37℃ for 1 h. For western blotting, the mixtures were quenched to terminate the reaction. For precipitation with Ni-NTA super flow beads (Qiagen, CA, USA), the reaction was incubated with beads and SH-SY5Y cell lysate and rotated at 4℃ for 30 min. The samples were analyzed by western blotting.

Site-directed point mutation

Each of four tyrosine residues of α-SYN was substituted to alanine using the KOD-Plus-Mutagenesis Kit (TOYOBO, Osaka, Japan). The point-mutated α-SYN, Y39A, Y125A, Y133A, Y136A, were phosphorylated in TKB1 competent cells except for the substituted site. A GST pull-down assay and western blot were performed with these GST-α-SYNs.

GST pull-down assay

GST-α-SYN was expressed in *E. coli* BL21 competent cells for the nonphosphorylated form and *E. coli* TKB1 competent cells (Stratagene, CA, USA) containing a plasmid expressing tyrosine kinase for the phosphorylated form. The transformed plasmid DNA was induced with 1 mM IPTG for 4h at 37℃. Harvested cells were lysed in PBS by sonication at 4℃, and crude cell

lysates were sedimented by centrifuge at 13,000 rpm for 10 min at 4℃. The supernatants obtained were quantified and used in a GST pull-down assay. The samples, including PBS washed GST beads (Glutathione Sepharose 4B, GE healthcare, UK) and bacterial cell lysate, were incubated with gentle rotation for 1 h at 4℃. GST protein-bound beads were washed three times with lysis buffer and incubated in the SH-SY5Y cell lysate with gentle rotation for 2 h at 4℃. The supernatant was discarded by centrifuge at 5,000 rpm for 30 sec and the beads were washed with lysis buffer. After SDS sample buffer was added to the beads, the samples were boiled for 5 min at 100℃, and then western blot was performed as described above.

Lysosome isolation and activity measurement

SH-SY5Y cells were trypsinized, and growth medium with 10% fetal bovine serum was added. The cells were centrifuged for 5 min at 600 x g. The cells were resuspended in ice cold PBS, counted and centrifuged for 5 min at 600 x g at 4℃. After repeating the wash step once again, 2.7 times the packed cell volume of extraction buffer (Lysosome isolation kit) was added. The cells were broken in a homogenizer and were centrifuged at 1,000 x g for 10 min. The supernatant was transferred to a new tube and was centrifuged at 20,000 x

g for 20 min. The supernatant was removed and the pellet was resuspended in extraction buffer. For assessment of intactness of the lysosome, the change of absorbance by the uptake of neutral red dye was measured at 460 nm and 510 nm using ELISA reader. The neutral red uptake can be calculated by subtracting the value obtained at 460nm from the value obtained at 510 nm.

WST-1 assay for cell viability assay

SH-SY5Y cells in a 96well plate were treated with PQ (1 mM), MG132 (5 μM), Cu^{++} (70 μM) and PTP1B inhibitor (0-10 μM) and were incubated for 24 h. After 10 μL of WST-1 reagent was added to each well, the cells were incubated for 3 h. The absorbance of the samples was measured using an ELISA reader at 450 nm.

Behavioral test using the Rotarod

Male 8- to10- week-old (20-25 g) C57BL6 mice were treated with PQ (30 mg/kg) by a single I.P. injection, once a week for 3 weeks. PTP1B inhibitor was dissolved in 95% ethanol and diluted with PBS for injection and administered by I.P. injection at a dose of 1 mg/kg, every 2 d and 3 h before the PQ injection for 3 weeks.

The motor coordination and fatigue resistance of the PD mouse model were measured using an accelerating Rotarod. Mice were conditioned three times at a

speed of 8 rpm for 1 min. After thirty minutes from the last conditioning, the locomotor activity of the mice was tested. The Rotarod test was started by placing the mouse on a rod and was stopped when mouse fell off the rod or 300 sec passed, whichever came first. The rotation speed was accelerated from 4 to 40 rpm gradually. Each mouse was subjected to 5 trials per day with 5 min interval between trials. Mice were housed one per cage on a 12:12 reversed light-dark cycles under controlled temperature (25℃) and proper humidity with free access to food and water. The mice were divided into 3 groups with 7 animals in each group.

Statistical analysis

Student's t-test and one-way ANOVA were performed using PASW statistics 18 (SPSS Inc., Chicago, IL, USA) to determine the relationships among the groups. Values of $P < 0.05$ (*), $P < 0.01$ (**), $P < 0.001$ (***) were considered to be significant.

RESULTS

Proteasomal dysfunction increases the binding of α-SYN to HSC70.

To verify the changes in the location of α-SYN, SH-SY5Y cells were treated with 1 μM of MG132 for 24 h. The cells were then stained with anti-α-SYN (green) antibody. To determine the lysosomal stability and CLS activation, the cells were co-stained with LysoTracker® (red). Under conditions of proteasomal dysfunction, lysosomes co-localized with α-SYN were increased (Fig. 1A). This result suggests that degradation via the lysosomal pathway is activated and that α-SYN is translocated into the activated lysosome, resulting from a blockage of the proteasomal degradation pathway.

It was also found that the binding between HSC70 and α-SYN was increased by treatment with 1 μM MG132 using immunoprecipitation by anti-HSC70 antibody. That binding was increased in the proteasome dysfunctional condition and the binding form of α-SYN was high molecular weight (Fig. 1B).

Therefore, to identify the status of high molecular weight α-SYN, The *in vitro* ubiquitination assay was performed and It was observed that ubiquitination of α-SYN increased its binding to HSC70. His-tagged α-SYN was ubiquitinated and precipitated by Ni-NTA resin after incubation with SH-SY5Y cell lysate.

Consequentially, it was identified that the amount of HSC70 bound to α-SYN was increased when it was ubiquitinated (Fig. 1C). Moreover, it was confirmed that the level of shifted α-SYN, corresponding to ubiquitination, and the level of HSC70 bound to α-SYN were increased with 1 μM MG132 treatment using immunoprecipitaion by anti-α-SYN antibody. And the phosphorylation of ubiquitinated α-SYN was increased when the proteasome was not functional (Fig. 1D).

In addition, It was determined that the phenomena by activated autopagy-lysosome system including increase of tyrosine phosphorylation and increase of the binding to HSC70 of α-SYN were similarly appeared to events by inhibition of ubiquitin-proteasome system. Activation of the lysosomal degradation pathway by starvation resulted in an activation of lysosomes and an increase of α-SYN binding to HSC70, which is rapidly degraded by the autophagy-lysosomal pathway (Fig. 2).

Tyrosine phosphorylation of α-SYN increases the binding of α-SYN to HSC70, and phosphorylation of Y136 is the most effective in promoting HSC70 binding.

To determine the important factors for binding between α-SYN and HSC70, tyrosine phosphorylated GST-α-SYN and nonphosphorylated GST-α-SYN were

prepared and used in a GST pull-down assay. PGEX4T1 plasmid vector expressing GST-α-SYN was transformed into BL21 competent cells for the nonphosphosrylated form or TKB1 competent cells for the tyrosine phosphorylated form. The transformed bacterial cells were grown in LB broth and induced with 1 mM of IPTG at 37℃ for 4 h. Nonphosphorylated α-SYN or tyrosine phosphorylated α-SYN purified with GST beads from bacterial cell lysates was incubated with SH-SY5Y cell lysate. The binding of HSC70 to tyrosine phosphorylated α-SYN was increased relative to nonphosphosrylated α-SYN (Fig. 3A). The HSC70 level bound with α-SYN was quantified using the Image J program and is shown in Fig. 3B.

Next, it was determined which among the four α-SYN tyrosine residues (Tyr39, Tyr125, Tyr133 and Tyr136) was most effective at promoting the binding between α-SYN and HSC70. After each tyrosine residue was substituted by alanine using the KOD-Plus-Mutagenesis Kit (Table1), GST pull-down assay was performed with the point-mutated α-SYN. Although tyrosine phosphorylation of α-SYN was decreased by dephosphorylation of Y125 and Y136, the binding of HSC70 was significantly decreased by dephosphorylation of Y136 (Fig. 3C). The intensity of each band was measured using the Image J program, and the results are shown in Fig. 3D.

Phosphorylation of focal adhesion kinase (FAK) was regulated by

MG132 and PTP1B inhibitor.

Western blot was performed with MG132 (1 μM)-treated SH-SY5Y cells to verify the tyrosine phosphorylation of FAK. Under this condition, α-SYN was changed to high molecular weight forms that are consistent with multi-ubiquitinated modification. Binding of α-SYN with HSC70 was also increased (Fig. 1B). In previous reports, it has been shown that the activity of FAK is secured by phosphorylation of the tyrosine 925 residue (47). Therefore, to calibrate the FAK activity, we used anti-phospho FAK antibody for the tyrosine 925 residue. The level of phosphorylated FAK at Y925 was increased by MG132 after 3 h (Fig. 4).

Ultimately, PTP1B was searched and chose for phosphatases that regulate FAK activity. Then, It was confirmed that in SH-SY5Y cells, the phosphorylation of FAK is increased in a time dependent fashion by treatment with PTP1B inhibitor, a specific membrane-permeable inhibitor of tyrosine phosphatase PTP1B (50 μM) (48) (Fig. 5). The phosphorylation of FAK at the tyrosine residue 925 was markedly increased at 30 min after treatment with PTP1B inhibitor.

PTP1B inhibitor and FAK regulated the phosphoryation of α-SYN and the binding of α-SYN to HSC70.

To clarify if the phosphorylation of α-SYN can be regulated by protein-tyrosine phosphatase (PTP) inhibitors and can affect the binding of α-SYN to HSC70 in SH-SY5Y cells, western blot and immunoprecipitation were performed with α-SYN antibody in SH-SY5Y cell lysates treated with PTP1B inhibitor (50 μM) or pervanadate (200 μM). Pervanadate, which is known to be a general protein-tyrosine phosphatase (PTP) inhibitor, is the complex of vanadate and hydrogen peroxide and is a commonly-used PTP inhibitor (49). As shown by Fig. 6A, tyrosine phosphorylation was observed, and the shifted size of α-SYN increased in a time-dependent manner. To identify of FAK as the kinase responsible for α-SYN phosphorylation, phosphorylated α-SYN was immunoprecipitated in the fak silenced or PTP1B inhibitor (50 μM, 30 min) treated SH-SY5Y cell lysates and immunoblotted with anti-phosphotyrosine and anti-α-SYN antibodies. The phosphorylated α-SYN was decreased by knock down of fak while the phosphorylated α-SYN was increased by PTP1B inhibitor. And, in fak silenced SH-SY5Y, PTP1B inhibitor could not induce the phosphorylation of α-SYN (Fig. 6A).

Also, when pervanadate was treated to SH-SY5Y, the binding of α-SYN with HSC70 was increased beginning 3 min after treatment. For the PTP1B inhibitor, the binding was increased beginning 5 min after treatment. It was also examined if the SHP1/2 PTP inhibitor affects the binding of α-SYN to HSC70. SHP1/2 PTP

inhibitor is a cell-permeable 7-aza-8-hydroxyquinoline compound known to act as a potent, catalytic site-targeting inhibitor of SHP-1 and SHP-2 protein tyrosine phosphatases. It was confirmed that SHP1/2 PTP inhibitor (50 μM) did not affect the binding of α-SYN to HSC70. The HSC70 bands were measured using the Image J program, and the results are shown in Fig. 6B.

PTP1B inhibitor decreased α–SYN aggregation in SH-SY5Y cells.

It was investigated if α-SYN aggregation can be reduced by treatment with PTP1B inhibitor and pervanadate under protein aggregation-induced conditions. SH-SY5Y cells were treated with PTP1B inhibitor (50 μM) or pervanadate (200 μM) for 24 h while under cellular stress produced by treatment with MG132 (1 μM). The levels of α-SYN and tyrosine phosphorylation were determined using western blotting. Tyrosine phosphorylation of α-SYN reduced the shifted α-SYN band and the monomeric α-SYN band (Fig. 7). The shifted α-SYN bands were also decreased by injection with PTP1B inhibitor in PQ-induced PD model (Fig. 10D)

PTP1B inhibitor increased the translocation of α-SYN into the lysosome.

To determine if translocation of α-SYN into the lysosome increased with tyrosine phosphorylation, crude fractions of lysosomes were isolated from SH-SY5Y cells treated with MG132 (1 μM) or both MG132 (1 μM) and PTP1B inhibitor (10 μM) by gradient centrifugation. The amount of α-SYN that translocated into the lysosome was increased and corresponded with the increase in tyrosine phosphorylation induced by the PTP1B inhibitor. The amount of HSC70 and LAMP-2A, but not the level of LAMP-1 and neprilysin, in the lysosomes was also increased by PTP1B inhibitor treatment (Fig. 8A). Neprilysin is a known substrate of lysosomes and was used to validate CLS activity. Moreover, the uptake of neutral red dye into the isolated lysosomes was calibrated for the lysosomal activity of each sample. The shift in the absorbance maximum (SAM) value of the neutral red dye from 460 nm to 510 nm under acidic conditions found in the lysosome is an indicator of lysosomal intactness and activity (Fig. 8B).

PTP1B inhibitor had protective effects against PQ, MG132 and Cu^{++} in SH-SY5Y cells.

Cell viability assays also were carried out to confirm the protective effect of the PTP1B inhibitor against cytotoxicity. SH-SY5Y cells were treated with PQ (1 mM), MG132 (5 μM) or Cu^{++} (70 μM) with the PTP1B inhibitor (0-10 μM) and

incubated for 24h. After the WST-1 reagent was added, the absorbance of each sample was measured using an ELISA reader. The viability of the cells was dose-dependently increased by co-treatment with the PTP1B inhibitor (Fig. 9A, 9B, 9C). However, the protection against cytotoxicity induced by Cu^{++} was less effective than protection against the other two conditions.

The effects of PTP1B inhibitor in PQ-induced PD mouse model.

To elucidate the effects of the PTP1B inhibitor in a PD mouse model, PD mouse model was prepared by injecting PQ. The mice were divided into three groups: the control group (CTL), the PQ-only injected group (PQ) and the PQ and PTP1B inhibitor-injected group (PQ/PTP1B inhibitor). PQ and PTP1B inhibitor were administered by I.P. injection for 3 weeks, and the behavioral test was performed in the fourth week. First, using immunohistochemistry, I determined if the PTP1B inhibitor had a protective effect in the dopaminergic neurons. The immunohistochemical analysis showed that TH-positive cells were significantly decreased in the PQ-injected group compared to the control group and were rescued in the PTP1B inhibitor-injected group (Fig. 10A). Fig. 10B showed the level of TH by measurement of Image J program. In addition, the effect of the PTP1B inhibitor was confirmed in behavioral performance using the rotarod test and the elevated body swing test. Rotarod performance was significantly

improved in the PTP1B inhibitor-injected group (Fig. 10C) but performance on the elevated body swing test was not. Moreover, to identify the level of α-SYN and TH in midbrain tissue lysate, Western blot analysis was performed. The increased level of α-SYN was decreased and the decreased level of TH was recovered by PTP1B inhibitor (Fig. 10D).

A

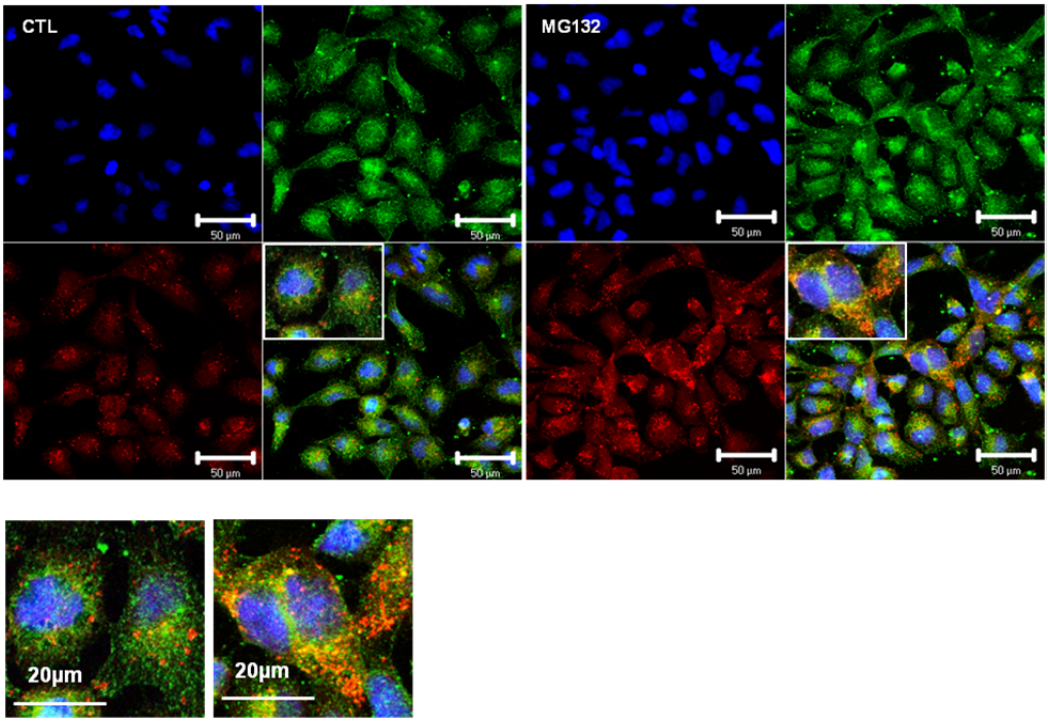

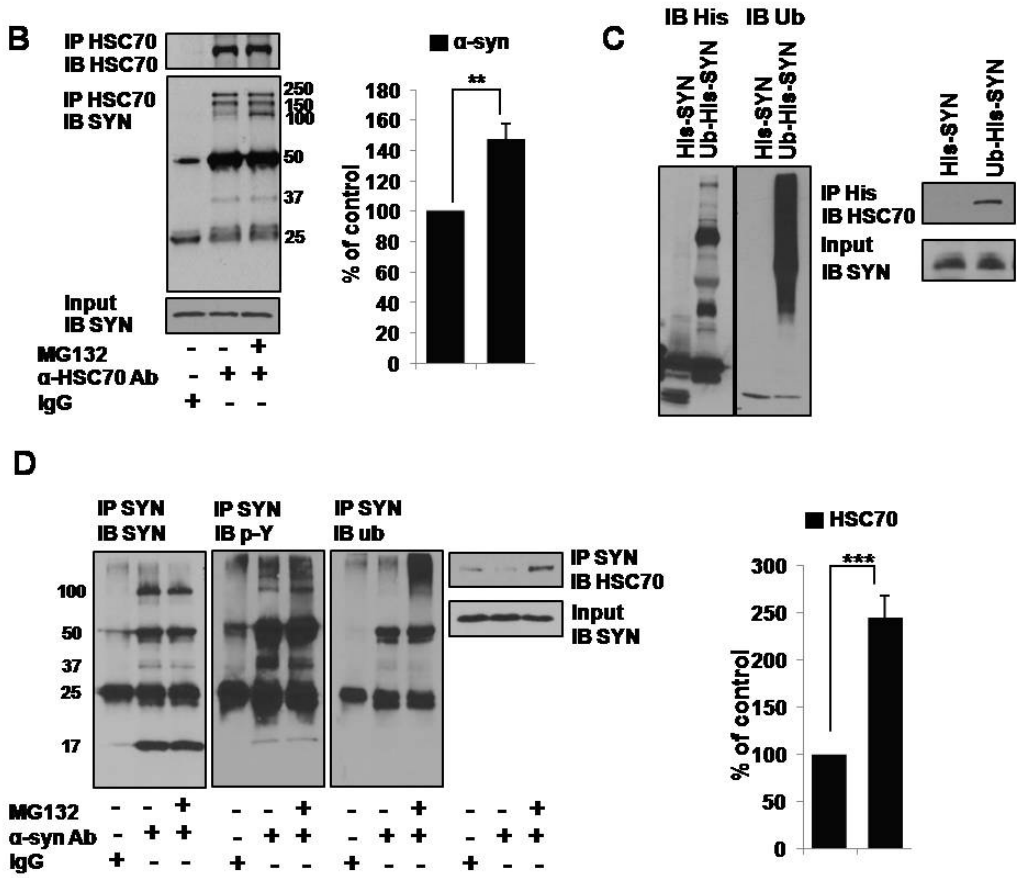

Figure1. Proteasomal dysfunction increased the binding of ub-α-SYN to HSC70. A. Lysosomal translocation of α-SYN. SH-SY5Y cells with or without MG132 (1 μM, 24 h) were detected with anti-α-SYN antibody (green), LysoTracker® (red) and DAPI (Blue) using confocal microscope. Scale bar = 20 μm. **B.** Immunoprecipitations with anti-HSC70 antibody in MG132 (1 μM) treated SH-SY5Y cells were probed with an anti-α-SYN or HSC70 antibody. Binding of

α-SYN with HSC70 was increased in lysosomal translocation condition. **C.** For *in vitro* ubiquitination assay, His-tagged recombinant α-SYN was ubiquitinated with Mg-ATP, ubiquitin, E1, E2 and E3 enzyme and blotted with anti-His or anti-ubiquitin antibodies. And binding with HSC70 was detected by Ni-NTA precipitation of His-SYN after incubation with SH-SY5Y cell lysate**.** Binding form of α-SYN with HSC70 was ubiquitinated but its affinity was weak. **D.** Immunoprecipitated Ub-α-SYN in SH-SY5Y was shown in western blot with phosphotyrosine, ubiquitin, hsc70, and α-SYN antibody. Phosphorylation of Ub-α-SYN appeared the strong binding with HSC70. $P < 0.01$ (**), $P < 0.001$ (***)

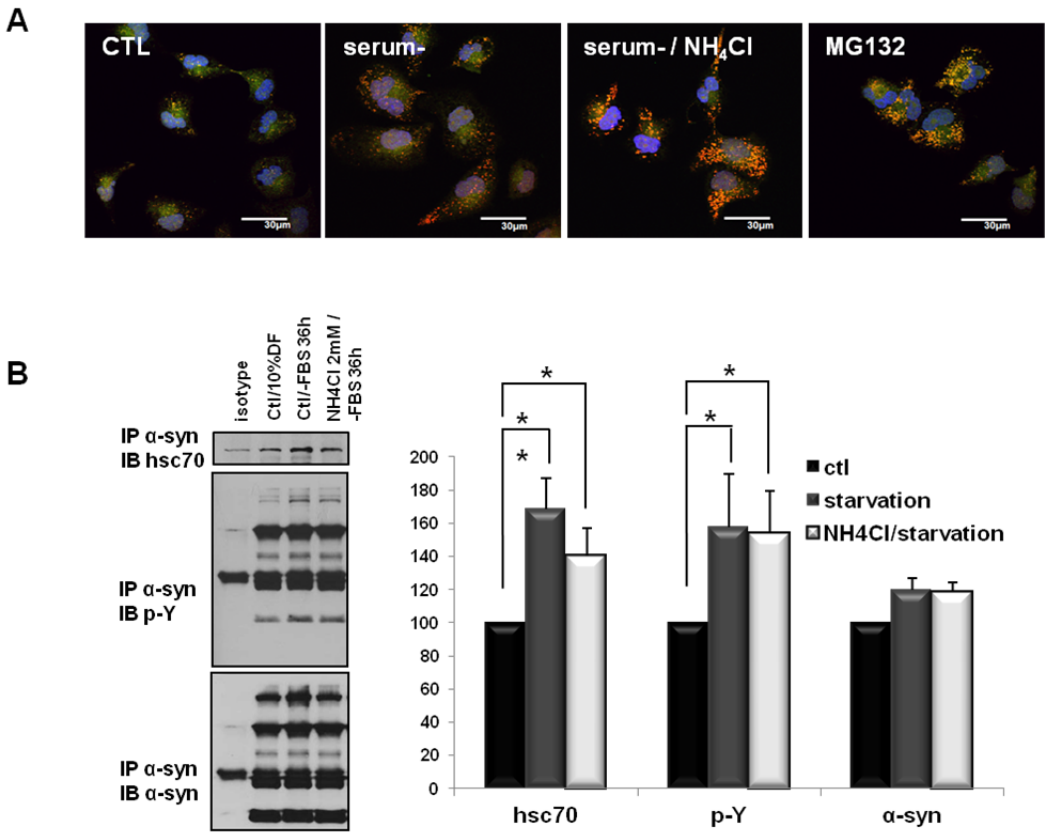

Figure2. The level of lysosome and the binding of α-SYN with HSC70 were increased in serum-starved condition. A. SH-SY5Y cells were cultured in serum-starved DMEM or treated with NH_4Cl (1 mM; 36 h) in serum-starved DMEM or treated with MG132 in DMEM contained 10 % FBS. The number and size of the lysosomes were increased in the serum-starved condition and

proteasome blocked condition by the immunocytochemistry. **B.** After immunoprecipitation was performed with anti-α-SYN antibody, the samples were identified by western blot analysis. The binding of α-SYN with HSC70 was increased in the autophagic condition induced by serum starvation (Fig. 2B). $P < 0.05$ (*), $P < 0.01$ (**)

A

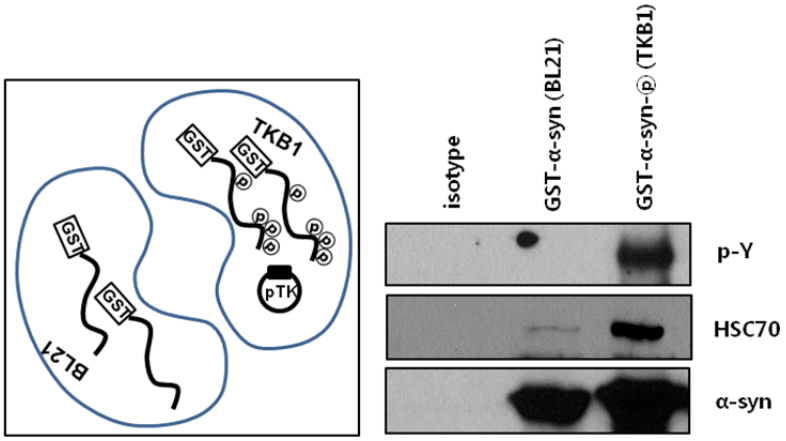
TKB1
GST
pTK
BL21
isotype
GST-α-syn (BL21)
GST-α-syn-ⓟ (TKB1)
p-Y
HSC70
α-syn

B

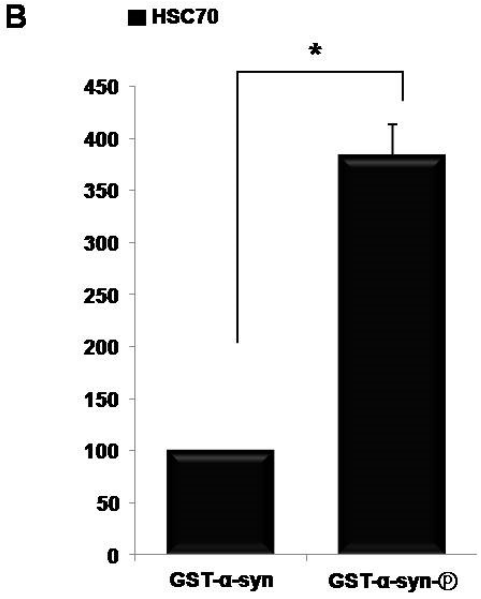
HSC70
*
450
400
350
300
250
200
150
100
50
0
GST-α-syn
GST-α-syn-ⓟ

C

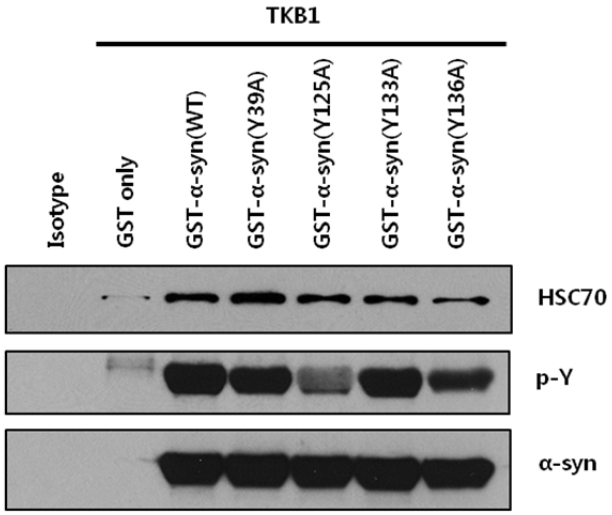
TKB1
Isotype
GST only
GST-α-syn(WT)
GST-α-syn(Y39A)
GST-α-syn(Y125A)
GST-α-syn(Y133A)
GST-α-syn(Y136A)
HSC70
p-Y
α-syn

D

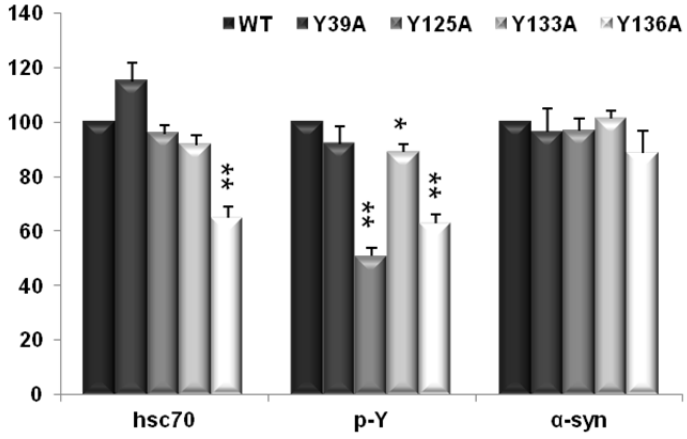
WT
Y39A
Y125A
Y133A
Y136A
140
120
100
80
60
40
20
0
**
**
*
**
hsc70
p-Y
α-syn

Figure3. Binding of α-SYN with HSC70 was increased by tyrosine phosphorylation. A. GST-α-SYN or tyrosine phosphorylated GST-α-SYN was expressed in *E.coli* BL21 or TKB1 competent cells containing a plasmid expressing tyrosine kinase. Each form of GST tagged α-SYN was isolated from bacterial cell lysates using GST beads and incubated in SH-SY5Y cell lysates. Precipitated samples by GST were examined using western blot analysis. The binding of α-SYN with HSC70 was increased by phosphorylation at all four of the tyrosine residues. **B.** The intensity of each band is represented by the graph. **C.** Each tyrosine residue of α-SYN was substituted by alanine using the KOD-Plus-Mutagenesis Kit. The GST pull-down assay and western blot analysis were performed with point mutated GST-α-SYN (Y39A, Y125A, Y133A and Y136A). **D.** The intensity of each band is represented by the graph. $P < 0.05$ (*), $P < 0.01$ (**)

Table1. Point mutation of α-SYN at tyrosine residues

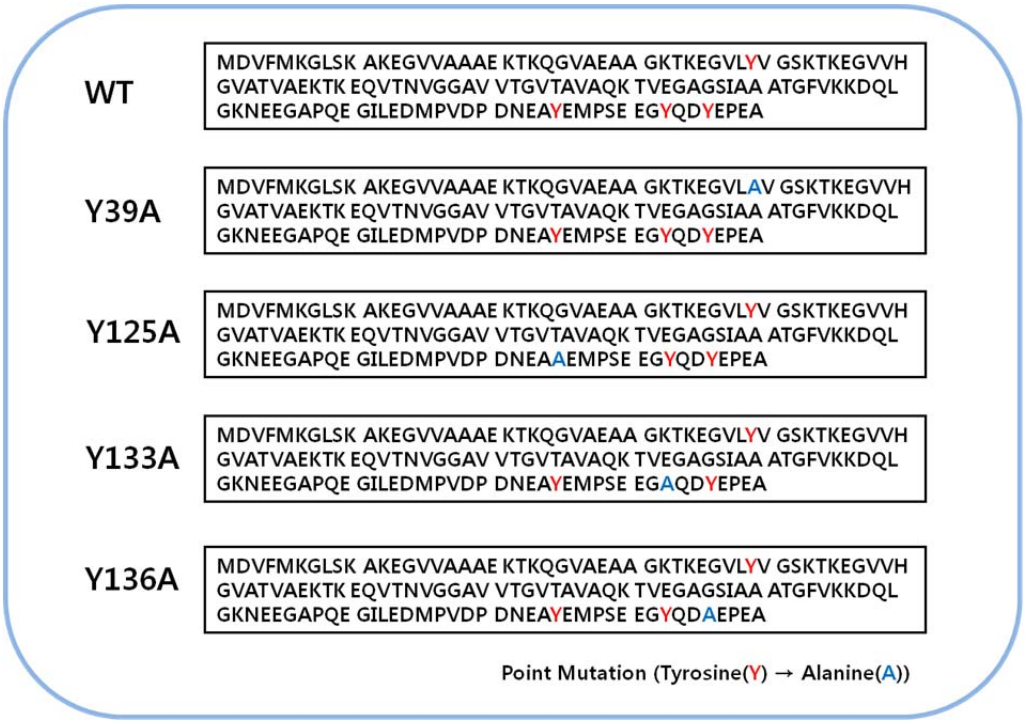

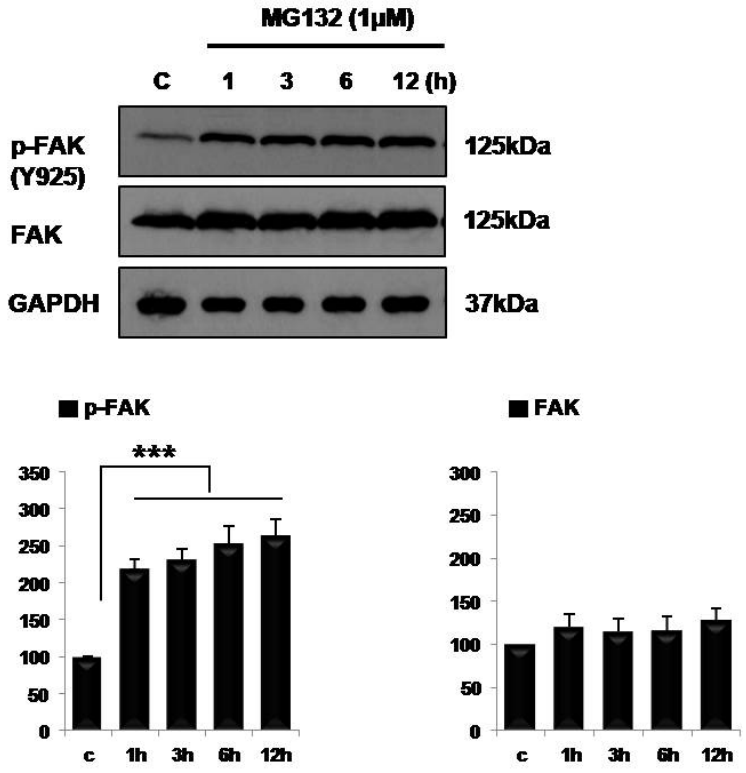

Figure4. Phosphorylation of FAK at Y925 was increased by MG132. The phosphorylation of FAK at Y925 was detected by western blot analysis. Increased FAK phosphorylation at Y925 was observed in SH-SY5Y cell lysate treated with MG132 (1 μM; 1, 3, 6, 12 and 24 h). The level of FAK expression was not affected by MG132. $P < 0.001$ (***)

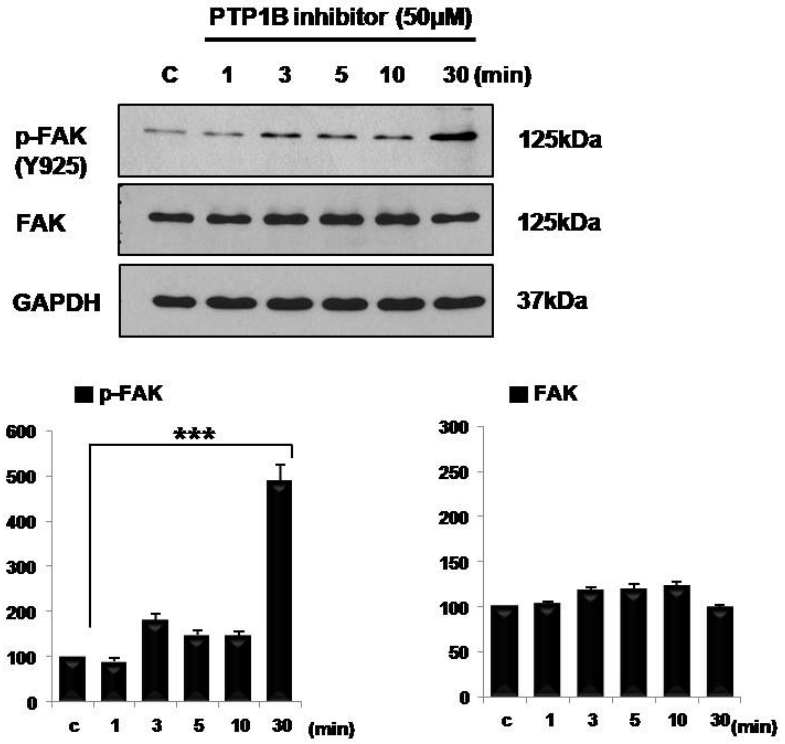

Figure5. Phosphorylation of FAK at Y925 was increased by PTP1B inhibitor.

SH-SY5Y cells were treated with PTP1B inhibitor (50 μM; 1, 3, 5, 10 and 30 min) and western blot was performed on the cell lysate. Phosphorylated FAK at Y925, not the FAK expression level, was remarkably increased by the PTP1B inhibitor after 30 min. $P < 0.001$ (***)

A

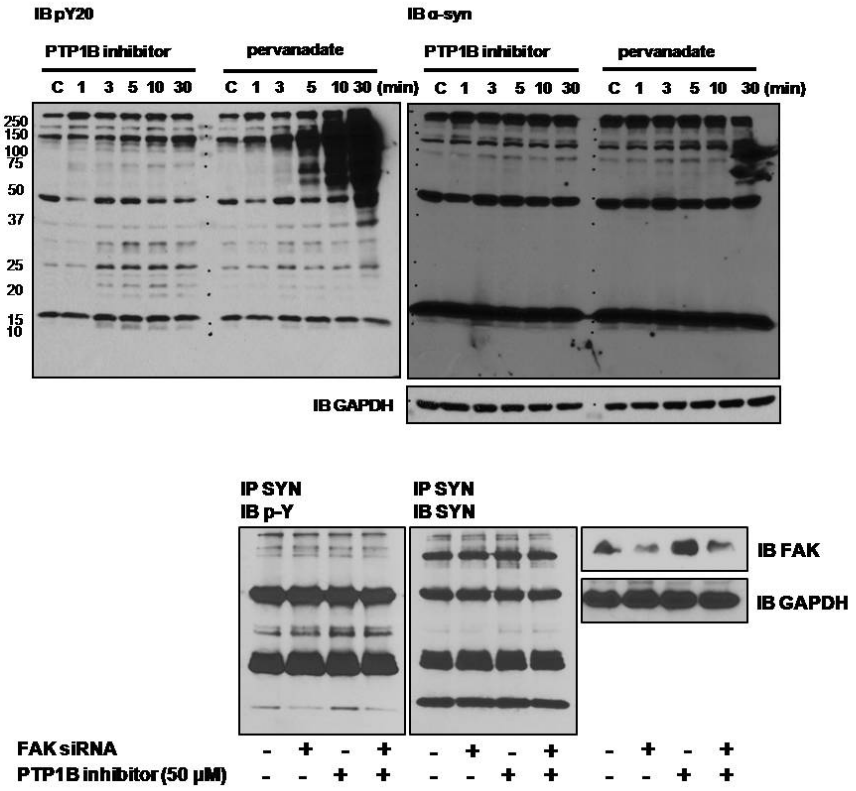
IB pY20
IB α-syn
PTP1B inhibitor
pervanadate
PTP1B inhibitor
pervanadate
C 1 3 5 10 30 C 1 3 5 10 30 (min)
C 1 3 5 10 30 C 1 3 5 10 30 (min)
250
150
100
75
50
37
25
20
15
10
IB GAPDH
IP SYN
IB p-Y
IP SYN
IB SYN
IB FAK
IB GAPDH
FAK siRNA - + - + - + - + - + - +
PTP1B inhibitor (50 μM) - - + + - - + + - - + +

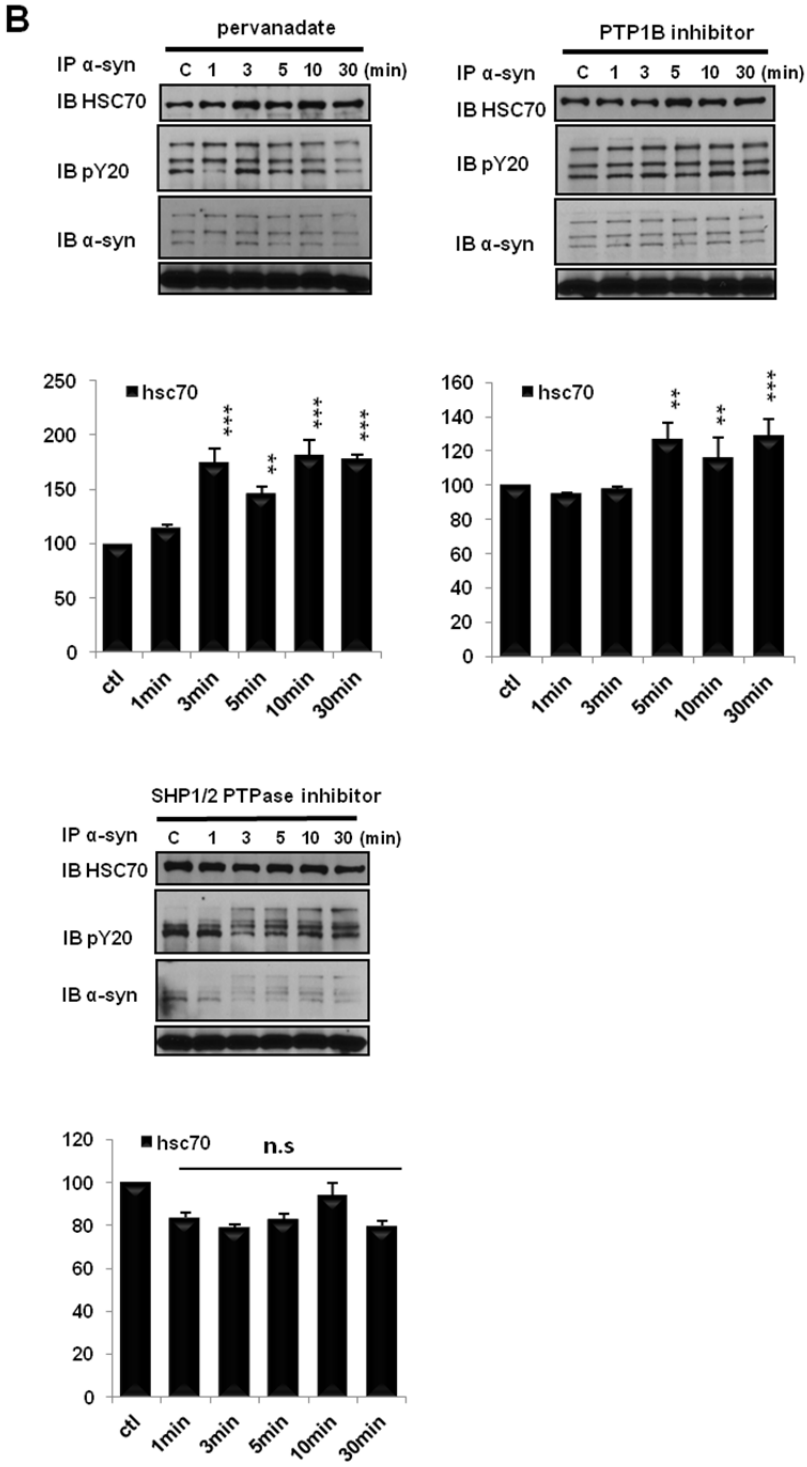
B
pervanadate
IP α-syn
C 1 3 5 10 30 (min)
IB HSC70
IB pY20
IB α-syn
PTP1B inhibitor
IP α-syn
C 1 3 5 10 30 (min)
IB HSC70
IB pY20
IB α-syn
hsc70
250
200
150
100
50
0
***
**
***
***
ctl
1min
3min
5min
10min
30min
hsc70
160
140
120
100
80
60
40
20
0
**
**
***
ctl
1min
3min
5min
10min
30min
SHP1/2 PTPase inhibitor
IP α-syn
C 1 3 5 10 30 (min)
IB HSC70
IB pY20
IB α-syn
hsc70
n.s
120
100
80
60
40
20
0
ctl
1min
3min
5min
10min
30min

Figure6. Phosphorylation at the tyrosine residues of α-SYN was regulated by PTP inhibitors and FAK and binding of α-SYN to HSC70 was increased by PTP inhibitors. A. SH-SY5Y cells treated with protein tyrosine phosphatase inhibitors (PTP1B inhibitor (50 μM) or pervanadate (200 μM)) and analyzed using western blot. Tyrosine phosphorylation of α-SYN was time dependently increased by treatment with inhibitors. Anti-GAPDH antibody was used for an equal protein loading control (Top). α-SYN was immunoprecipitated in fak silenced or PTP1B inhibitor (50 μM, 30 min) treated SH-SY5Y cell lysate and immunoblotted with anti-phosphotyrosine and anti-α-SYN antibodies. The phosphorylated α-SYN was decreased by silencing of fak and increased by PTP1B inhibitor treatment. In fak silenced SH-SY5Y, the phosphorylation of α-SYN was not induced by PTP1B inhibitor treatment). **B.** Immunoprecipitation was carried out with anti-α-SYN antibody in protein tyrosine phosphatase inhibitor-treated SH-SY5Y cell lysates (PTP1B inhibitor (50 μM) or pervanadate (200 μM) or SHP1/2 PTPase inhibitor (50 μM)). The binding between α-SYN and HSC70 was time dependently increased in PTP1B inhibitor- or pervanadate-treated samples. $P < 0.01$ (**), $P < 0.001$ (***)

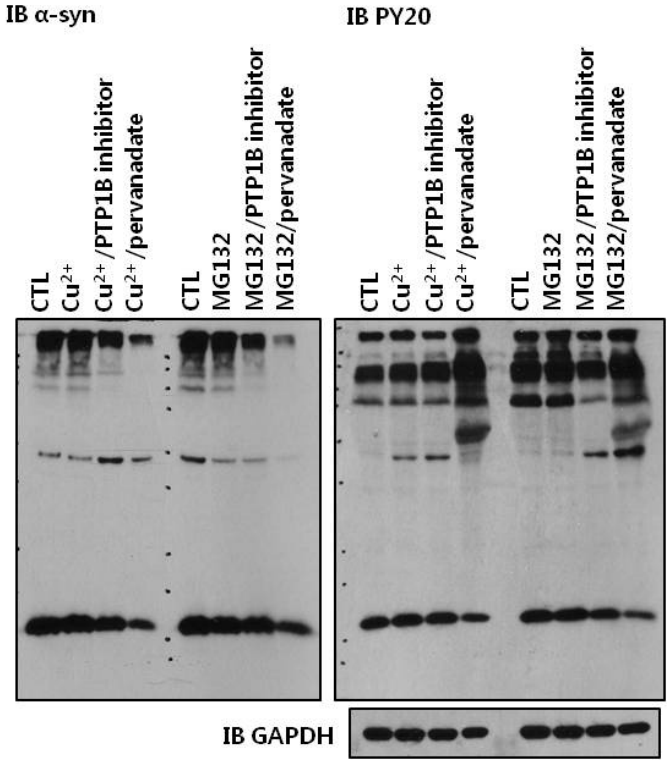

Figure7. PTP1B inhibitor decreased α-SYN aggregates in SH-SY5Y cells. SH-SY5Y cells were treated with MG132 (1 μM; 24h), Cu^{++} (7 μM; 24h) and PTP inhibitors (PTP1B inhibitor (50 μM) or pervanadate (200 μM)) and western blot analysis was performed. Monomeric α-SYN and size-shifted α-SYN was decreased along with increased phosphorylation at the tyrosine residues of α-SYN in the proteasome-inhibited condition.

A

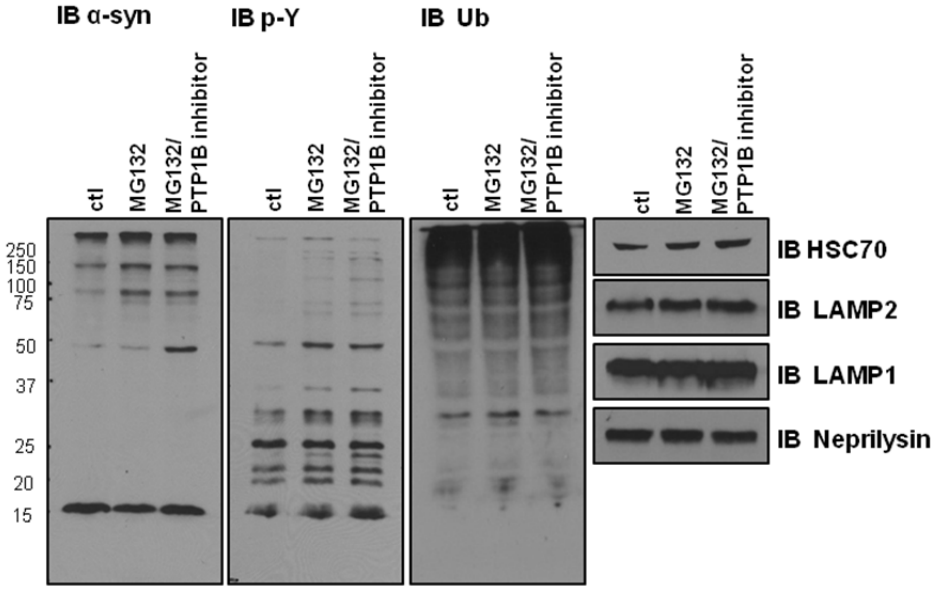
IB α-syn
IB p-Y
IB Ub
ctl
MG132
MG132/ PTP1B inhibitor
250
150
100
75
50
37
25
20
15
IB HSC70
IB LAMP2
IB LAMP1
IB Neprilysin

B

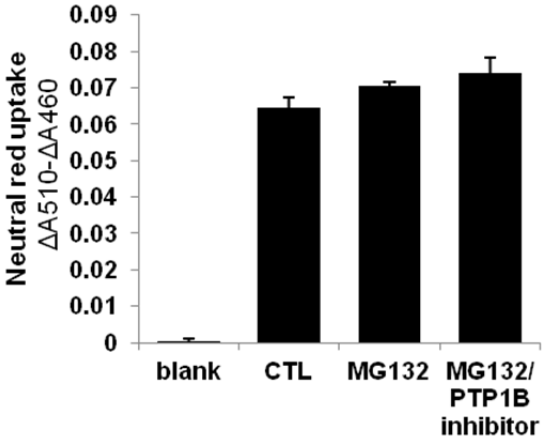
Neutral red uptake
ΔA510-ΔA460
0.09
0.08
0.07
0.06
0.05
0.04
0.03
0.02
0.01
0
blank
CTL
MG132
MG132/ PTP1B inhibitor

Figure8. PTP1B inhibitor increased the translocation of α-SYN into the lysosome. A. SH-SY5Y cells were treated with MG132 (1 μM) only or in the presence of both MG132 and PTP1B inhibitor (10 μM). The cells were broken by a homogenator. The crude lysosome fraction was isolated by centrifugation and analyzed by western blotting. The amount of α-SYN that translocated into the lysosome was increased by the PTP1B inhibitor. The levels of HSC70 and LAMP-2A, but not neprilysin, were also increased. LAMP-1 was used as the protein loading control. **B.** The shift in absorbance following neutral red dye uptake in each sample was measured at 460 nm and 510 nm using an ELISA reader.

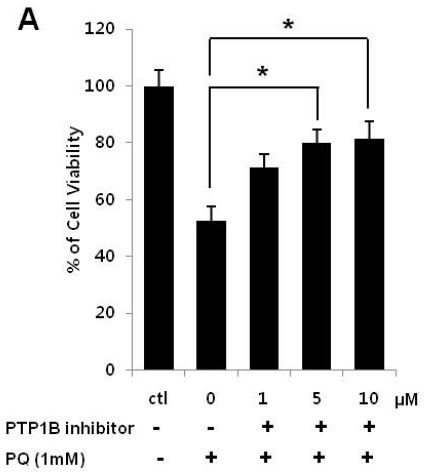
A
120
100
80
60
40
20
0
% of Cell Viability
*
*
ctl
0
1
5
10
μM
PTP1B inhibitor - - + + +
PQ (1mM) - + + + +

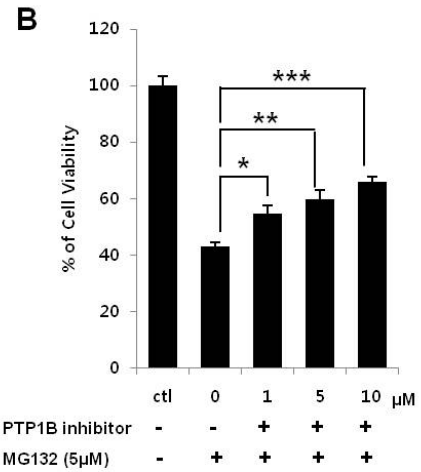
B
120
100
80
60
40
20
0
% of Cell Viability
***
**
*
ctl
0
1
5
10
μM
PTP1B inhibitor - - + + +
MG132 (5μM) - + + + +

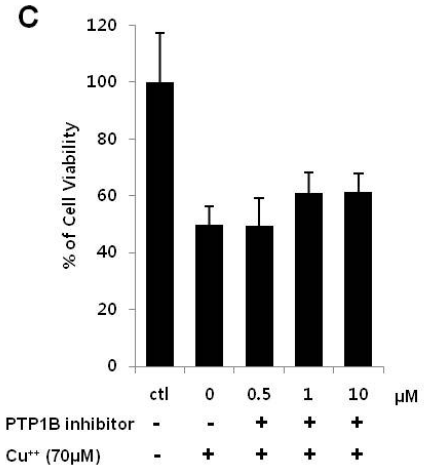
C
120
100
80
60
40
20
0
% of Cell Viability
ctl
0
0.5
1
10
μM
PTP1B inhibitor - - + + +
Cu++ (70μM) - + + + +

Figure9. PTP1B inhibitor had protective effects against cytotoxicity induced by PQ, MG132 and Cu^{++} in SH-SY5Y cells. A. Cell viability assay was performed with PQ (1 mM) and PTP1B inhibitor (1-10 μM)-treated SH-SY5Y cells, and the absorbance was determined using an ELISA reader at 450 nm. The cells were protected from PQ-induced cytotoxicity by treatment with PTP1B inhibitor. PTP1B inhibitor has a protective effect against MG132 (**B)** or Cu^{++} (**C**)-induced cytotoxicity. $P < 0.05$ (*), $P < 0.01$ (**), $P < 0.001$ (***)

A

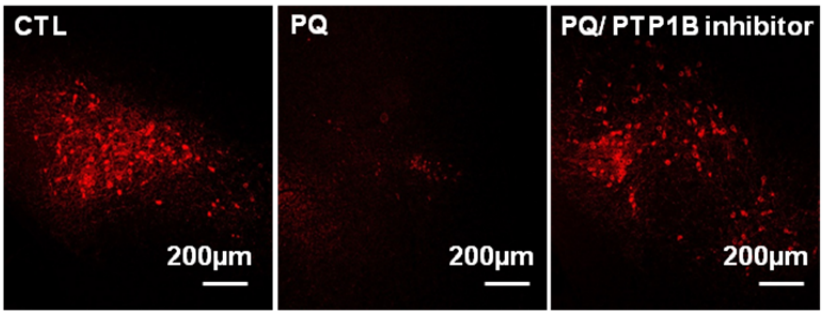
CTL
200μm
PQ
200μm
PQ/ PTP1B inhibitor
200μm

B

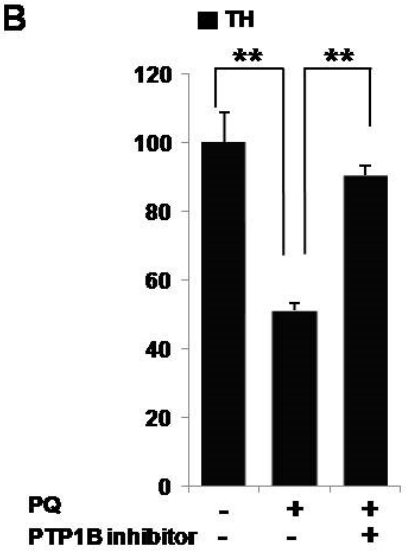
TH
**
**
120
100
80
60
40
20
0
PQ
-
+
+
PTP1B inhibitor
-
-
+

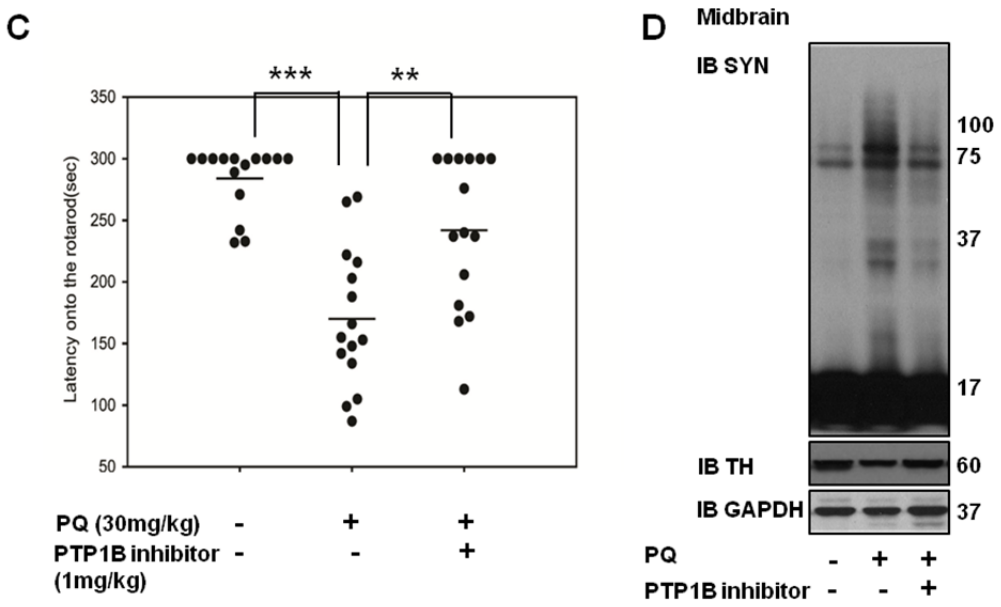

Figure10. PTP1B inhibitor increased neuronal survival and improved motor performance in PQ-induced PD model. A. For immunostaining, the tissue slices were incubated with anti-tyrosine hydroxylase (TH) antibody and observed using a confocal microscope. TH positive dopaminergic neuronal cells were increased in the PQ and PTP1B inhibitor co-injected group. Scale bar = 200 μm. **B.** The level of TH positive cells is shown by quantitative graph. **C.** PQ and PTP1B inhibitor were given by I.P. injection for 3 weeks, and the Rotarod test was performed in the fourth week. Rotarod performance was improved in the PQ and PTP1B

inhibitor co-injected group. **D.** The α-SYN and TH level was confirmed using western blot. While the level of α-SYN was increased in the PQ injected group and decreased in the PTP1B co-injected group, the level of TH was decreased in the PQ injected group and rescued in the PTP1B inhibitor co-injected group. $P < 0.05$ (*), $P < 0.01$ (**), $P < 0.001$ (***)

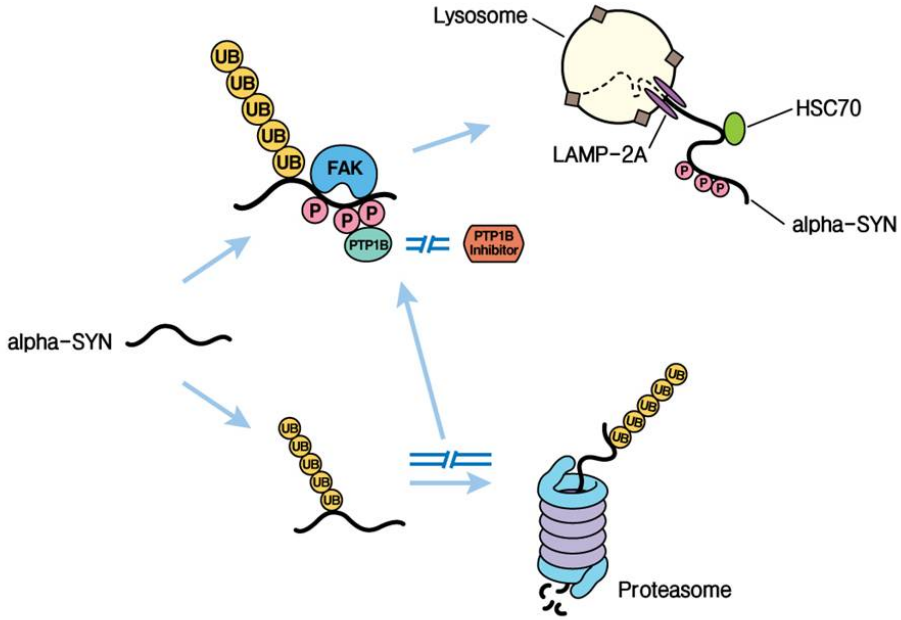

Figure11. Tyrosine phosphorylation of α-SYN is a crucial factor for the compensation of proteasome dysfunction. α-SYN can be degraded by the proteasome with ubiquitin or by the lysosome with HSC70. When α-SYN cannot be removed because of proteasomal dysfunction during cellular stress, tyrosine phosphorylation of α-SYN at Y136 by FAK under the influence of PTP1B inhibitor can be an important factor for compensatory degradation by the lysosomal pathway.

DISCUSSION

Many studies have already reported that α-SYN can be degraded not only by the ubiquitin-proteasomal pathway but also by the chaperone-lysosomal pathway (50, 51). I found that when the ubiquitin-proteasomal pathway was blocked by treatment with MG132, lysosomes were activated, α-SYN could translocate into activated lysosomes and the binding of α-SYN to HSC70 was increased. The key modifications that determine the binding between α-SYN and HSC70 have not been well characterized. Only the pentapeptide binding motif in the α-SYN sequence has been studied. To elucidate the crucial factors involved in the degradation pathway of α-SYN, I determined the relationship between the phosphorylation of tyrosine residues of α-SYN and its binding to HSC70. In my study, the binding of α-SYN and HSC70 was increased when the tyrosine residues of α-SYN were phosphorylated. These results suggest that tyrosine phosphorylation of α-SYN is an essential factor regulating the binding of α-SYN to HSC70. Many studies have shown that the 4 tyrosine residues (Tyr39, Tyr125, Tyr133 and Tyr136) of α-SYN can be phosphorylated (43, 44). My point mutation study also indicated that among four tyrosine residues, Y136 in the c-terminal of α-SYN is the most important site for the binding of α-SYN with HSC70 (Fig. 3C). In human and mouse brain, α-SYN aggregates contained the c-terminal truncated form (52). Also, multiple tyrosine phosphorylations in the c-terminal segment of

α-SYN prevent eosin-induced oligomerization (36). Therefore, it has been proposed that the c-terminus of α-SYN may have an important role in its clearance mechanisms.

First, the phosphorylation of α-SYN at Ser129 was investigated as the predominant modification of α-SYN, which is the key event responsible for Lewy body formation. It could be phosphorylated by some protein kinases, including casein kinase1 (CK1), casein kinase2 (CK2) or G-protein coupled receptor kinases at Ser129 (53-55). However, recently, the importance of tyrosine phosphorylation of α-SYN in the regulation of many cellular processes has been highlighted. Phosphorylated α-SYN at Ser129 has not been observed under normal physiological conditions but has been shown to be a significant pathological event in synucleinopathy brains (55). Phosphorylation at tyrosine residues has an effect on neurotoxicity (36, 46, 56). The tyrosine residues of α-SYN are phosphorylated by the Src family of protein-tyrosine kinases (PTKs) such as Fyn and c-Src and Syk (36, 43). In particular, the Tyr125 site is primarily phosphorylated by the Src family (43), and Tyr125 phosphorylation decreases in the aged brains of humans and flies (46).

To discover the Y136-related kinase, kinases were listed by protein interaction prediction sites [PIPS (http://www.compbio.dundee.ac.uk/ www-pips/) or PRISM (http://prism.ccbb.ku.edu.tr/prism/)], and the results contained CAM kinase II, protein kinase C, Fyn kinase, pp58, tyrosine kinase c-Src, FAK, pp60 (src),

MKNK2 and the receptor for activated C kinase (RACK1).

Also, I tested several kinase inhibitors including an inhibitor of Rhoa/ROCK-II, PRK2, MSK1, Rsk2/MAPKAP-K1b, an inhibitor of S6 kinase 1, MSK1, PKA, Rhoa /ROCK-II, Akt1/PKB, Rsk2/MAPKAP-K1b, an inhibitor of PRAK, MAPKAP-K2 5, PKCd, an inhibitor of MEK1/MEK2, MKK1, PRAK, p38/SAPK2a, Akt1/PKBa, an inhibitor of p38a/SAPK2a, p38a/SAPK2b, an inhibitor of PI3 kinase, Casein kinase 2, a Rsk2/MAPKAP-K1b, MSK1 inhibitor, a ROKa/ROCK II, PRK2, MSK1, Rsk2, PKA, p70 S6 Kinase, CaM Kinase, MLCK inhibitor and a MEK1 inhibitor Among the kinases tested, the focal adhesion kinase pp125 (FAK) was the most effective at α-SYN Y136. Because most of the kinases involved are in the src kinase family, src-associated phosphatases were searched and examined using inhibitors of SHP-1/SHP-2, PTP1B, CD45, PTPα, LAR, CDC 25 and PTPN1. I determined that the target phosphatase which dephosphorylates α-SYN was PTP1B. To confirm the effect of phosphatases on the phosphosrylation of α-SYN, first, I checked the phosphorylation of α-SYN in SH-SY5Y cells treated by pervanadate, a broadly used src-related phosphatase inhibitor, and the PTP1B inhibitor. Phosphorylation of α-SYN was time dependently increased by treatment with pervanadate and the PTP1B inhibitor.

The roles of PTP1B and FAK have been investigated in the integrin signaling pathway (57, 58). In my study, the PTP1B inhibitor affects tyrosine

phosphorylation of α-SYN and FAK. Tyrosine phosphorylation of FAK was increased by PTP1B inhibitor or by MG132 in SH-SY5Y cells. And the level of phosphorylated α-SYN was decreased in the fak silenced SH-SY5Y cells and PTP1B inhibitor cannot induce the phosphorylation of α-SYN without FAK. According to the results, I suggest that FAK is directly related to the phosphorylation of α-SYN and retainment of FAK activity by PTP1B inhibitor brought about the phosphorylation of α-SYN, increased binding of α-SYN to HSC70 and continuous movement into lysosomal compartment of α-SYN.

I anticipated that when the efficient removal of α-SYN is accomplished, the progress of PD can be delayed. When α-SYN aggregates were induced by copper or MG132, the levels of shifted and monomeric α-SYN were decreased according to the increase in tyrosine phosphorylation of α-SYN by pervanadate or the PTP1B inhibitor. Therefore, I concluded that the decreased level of α-SYN was the result of translocation into lysosome for degradation (Fig. 8), and long-term treatment with PTP1B inhibitor increased neuronal survival in PQ, MG132 and copper ion-treated cells (Fig. 9). Also, PTP1B inhibitor treatment protects dopaminergic neurons against cell death in a PQ-induced PD model. Moreover, the motor balance and coordination of the mice was improved in the PTP1B inhibitor injected group.

Taken together, these experiments provide a new direction for PD therapeutic targets: the regulation of α-SYN phosphorylation at Y136. Briefly, ubiquitinated

α-SYN is normally degraded by the proteasome, but during proteasomal dysfunction, α-SYN can be degraded by the lysosome through binding of α-SYN phosphorylated at Y136 to HSC70 (Fig. 11). In conclusion, I suggest that tyrosine phosphorylation of α-SYN can regulate the removal of α-SYN through enhanced lysosomal degradation of α-SYN and can decrease neuronal death in the early stage of PD. Furthermore, the PTP1B inhibitor can potentially be applied as a therapeutic agent for PD.

REFERENCES

1. Forno LS. Neuropathology of Parkinson's disease. Journal of neuropathology and experimental neurology. 1996;55(3):259-72.

2. Olanow CW, Tatton WG. Etiology and pathogenesis of Parkinson's disease. Annual review of neuroscience. 1999;22:123-44.

3. Goedert M. Familial Parkinson's disease. The awakening of alpha-synuclein. Nature. 1997;388(6639):232-3.

4. Bennett MC, Bishop JF, Leng Y, Chock PB, Chase TN, Mouradian MM. Degradation of alpha-synuclein by proteasome. The Journal of biological chemistry. 1999;274(48):33855-8.

5. Webb JL, Ravikumar B, Atkins J, Skepper JN, Rubinsztein DC. Alpha-Synuclein is degraded by both autophagy and the proteasome. The Journal of biological chemistry. 2003;278(27):25009-13.

6. Cuervo AM, Stefanis L, Fredenburg R, Lansbury PT, Sulzer D. Impaired degradation of mutant alpha-synuclein by chaperone-mediated autophagy. Science. 2004;305(5688):1292-5.

7. Pan T, Kondo S, Le W, Jankovic J. The role of autophagy-lysosome pathway in neurodegeneration associated with Parkinson's disease. Brain : a journal of neurology. 2008;131(Pt 8):1969-78.

8. McNaught KS, Olanow CW. Proteolytic stress: a unifying concept for the etiopathogenesis of Parkinson's disease. Annals of neurology. 2003;53 Suppl

3:S73-84; discussion S-6.

9. McNaught KS, Perl DP, Brownell AL, Olanow CW. Systemic exposure to proteasome inhibitors causes a progressive model of Parkinson's disease. Annals of neurology. 2004;56(1):149-62.

10. Bedford L, Hay D, Devoy A, Paine S, Powe DG, Seth R, et al. Depletion of 26S proteasomes in mouse brain neurons causes neurodegeneration and Lewy-like inclusions resembling human pale bodies. The Journal of neuroscience : the official journal of the Society for Neuroscience. 2008;28(33):8189-98.

11. Keck S, Nitsch R, Grune T, Ullrich O. Proteasome inhibition by paired helical filament-tau in brains of patients with Alzheimer's disease. Journal of neurochemistry. 2003;85(1):115-22.

12. Shringarpure R, Grune T, Sitte N, Davies KJ. 4-Hydroxynonenal-modified amyloid-beta peptide inhibits the proteasome: possible importance in Alzheimer's disease. Cellular and molecular life sciences : CMLS. 2000;57(12):1802-9.

13. Lopez Salon M, Pasquini L, Besio Moreno M, Pasquini JM, Soto E. Relationship between beta-amyloid degradation and the 26S proteasome in neural cells. Experimental neurology. 2003;180(2):131-43.

14. Bence NF, Sampat RM, Kopito RR. Impairment of the ubiquitin-proteasome system by protein aggregation. Science. 2001;292(5521):1552-5.

15. Jana NR, Zemskov EA, Wang G, Nukina N. Altered proteasomal function

due to the expression of polyglutamine-expanded truncated N-terminal huntingtin induces apoptosis by caspase activation through mitochondrial cytochrome c release. Human molecular genetics. 2001;10(10):1049-59.

16. Waelter S, Boeddrich A, Lurz R, Scherzinger E, Lueder G, Lehrach H, et al. Accumulation of mutant huntingtin fragments in aggresome-like inclusion bodies as a result of insufficient protein degradation. Molecular biology of the cell. 2001;12(5):1393-407.

17. Lee M, Hyun DH, Halliwell B, Jenner P. Effect of overexpression of wild-type and mutant Cu/Zn-superoxide dismutases on oxidative stress and cell death induced by hydrogen peroxide, 4-hydroxynonenal or serum deprivation: potentiation of injury by ALS-related mutant superoxide dismutases and protection by Bcl-2. Journal of neurochemistry. 2001;78(2):209-20.

18. Urushitani M, Kurisu J, Tsukita K, Takahashi R. Proteasomal inhibition by misfolded mutant superoxide dismutase 1 induces selective motor neuron death in familial amyotrophic lateral sclerosis. Journal of neurochemistry. 2002;83(5):1030-42.

19. Kristiansen M, Deriziotis P, Dimcheff DE, Jackson GS, Ovaa H, Naumann H, et al. Disease-associated prion protein oligomers inhibit the 26S proteasome. Molecular cell. 2007;26(2):175-88.

20. Tanaka K, Suzuki T, Hattori N, Mizuno Y. Ubiquitin, proteasome and parkin. Biochimica et biophysica acta. 2004;1695(1-3):235-47.

21. Yu WH, Dorado B, Figueroa HY, Wang L, Planel E, Cookson MR, et al.

Metabolic activity determines efficacy of macroautophagic clearance of pathological oligomeric alpha-synuclein. The American journal of pathology. 2009;175(2):736-47.

22. Cuervo AM, Bergamini E, Brunk UT, Droge W, Ffrench M, Terman A. Autophagy and aging: the importance of maintaining "clean" cells. Autophagy. 2005;1(3):131-40.

23. Klionsky DJ. The molecular machinery of autophagy: unanswered questions. Journal of cell science. 2005;118(Pt 1):7-18.

24. Shintani T, Klionsky DJ. Autophagy in health and disease: a double-edged sword. Science. 2004;306(5698):990-5.

25. Vogiatzi T, Xilouri M, Vekrellis K, Stefanis L. Wild type alpha-synuclein is degraded by chaperone-mediated autophagy and macroautophagy in neuronal cells. The Journal of biological chemistry. 2008;283(35):23542-56.

26. Mizushima N, Levine B, Cuervo AM, Klionsky DJ. Autophagy fights disease through cellular self-digestion. Nature. 2008;451(7182):1069-75.

27. Dice JF. Chaperone-mediated autophagy. Autophagy. 2007;3(4):295-9.

28. Dice JF. Peptide sequences that target cytosolic proteins for lysosomal proteolysis. Trends in biochemical sciences. 1990;15(8):305-9.

29. Mak SK, McCormack AL, Manning-Bog AB, Cuervo AM, Di Monte DA. Lysosomal degradation of alpha-synuclein in vivo. The Journal of biological

chemistry. 2010;285(18):13621-9.

30. Klionsky DJ, Emr SD. Autophagy as a regulated pathway of cellular degradation. Science. 2000;290(5497):1717-21.

31. Levine B, Klionsky DJ. Development by self-digestion: molecular mechanisms and biological functions of autophagy. Developmental cell. 2004;6(4):463-77.

32. Hideshima T, Bradner JE, Chauhan D, Anderson KC. Intracellular protein degradation and its therapeutic implications. Clinical cancer research : an official journal of the American Association for Cancer Research. 2005;11(24 Pt 1):8530-3.

33. Di Fonzo A, Chien HF, Socal M, Giraudo S, Tassorelli C, Iliceto G, et al. ATP13A2 missense mutations in juvenile parkinsonism and young onset Parkinson disease. Neurology. 2007;68(19):1557-62.

34. Meredith GE, Totterdell S, Petroske E, Santa Cruz K, Callison RC, Jr., Lau YS. Lysosomal malfunction accompanies alpha-synuclein aggregation in a progressive mouse model of Parkinson's disease. Brain research. 2002;956(1):156-65.

35. Chen L, Feany MB. Alpha-synuclein phosphorylation controls neurotoxicity and inclusion formation in a Drosophila model of Parkinson disease. Nature neuroscience. 2005;8(5):657-63.

36. Negro A, Brunati AM, Donella-Deana A, Massimino ML, Pinna LA.

Multiple phosphorylation of alpha-synuclein by protein tyrosine kinase Syk prevents eosin-induced aggregation. The FASEB journal : official publication of the Federation of American Societies for Experimental Biology. 2002;16(2):210-2.

37. Paik SR, Shin HJ, Lee JH. Metal-catalyzed oxidation of alpha-synuclein in the presence of Copper(II) and hydrogen peroxide. Archives of biochemistry and biophysics. 2000;378(2):269-77.

38. Yu Z, Xu X, Xiang Z, Zhou J, Zhang Z, Hu C, et al. Nitrated alpha-synuclein induces the loss of dopaminergic neurons in the substantia nigra of rats. PloS one. 2010;5(4):e9956.

39. Giasson BI, Duda JE, Murray IV, Chen Q, Souza JM, Hurtig HI, et al. Oxidative damage linked to neurodegeneration by selective alpha-synuclein nitration in synucleinopathy lesions. Science. 2000;290(5493):985-9.

40. Dorval V, Fraser PE. Small ubiquitin-like modifier (SUMO) modification of natively unfolded proteins tau and alpha-synuclein. The Journal of biological chemistry. 2006;281(15):9919-24.

41. Nonaka T, Iwatsubo T, Hasegawa M. Ubiquitination of alpha-synuclein. Biochemistry. 2005;44(1):361-8.

42. Shimura H, Schlossmacher MG, Hattori N, Frosch MP, Trockenbacher A, Schneider R, et al. Ubiquitination of a new form of alpha-synuclein by parkin from human brain: implications for Parkinson's disease. Science. 2001;293(5528):263-9.

43. Ellis CE, Schwartzberg PL, Grider TL, Fink DW, Nussbaum RL. alpha-synuclein is phosphorylated by members of the Src family of protein-tyrosine kinases. The Journal of biological chemistry. 2001;276(6):3879-84.

44. Nakamura T, Yamashita H, Takahashi T, Nakamura S. Activated Fyn phosphorylates alpha-synuclein at tyrosine residue 125. Biochemical and biophysical research communications. 2001;280(4):1085-92.

45. Mbefo MK, Paleologou KE, Boucharaba A, Oueslati A, Schell H, Fournier M, et al. Phosphorylation of synucleins by members of the Polo-like kinase family. The Journal of biological chemistry. 2010;285(4):2807-22.

46. Chen L, Periquet M, Wang X, Negro A, McLean PJ, Hyman BT, et al. Tyrosine and serine phosphorylation of alpha-synuclein have opposing effects on neurotoxicity and soluble oligomer formation. The Journal of clinical investigation. 2009;119(11):3257-65.

47. Basuroy S, Dunagan M, Sheth P, Seth A, Rao RK. Hydrogen peroxide activates focal adhesion kinase and c-Src by a phosphatidylinositol 3 kinase-dependent mechanism and promotes cell migration in Caco-2 cell monolayers. American journal of physiology Gastrointestinal and liver physiology. 2010;299(1):G186-95.

48. Huyer G, Liu S, Kelly J, Moffat J, Payette P, Kennedy B, et al. Mechanism of inhibition of protein-tyrosine phosphatases by vanadate and pervanadate. The Journal of biological chemistry. 1997;272(2):843-51.

49. Hebert Chatelain E, Dupuy JW, Letellier T, Dachary-Prigent J. Functional

impact of PTP1B-mediated Src regulation on oxidative phosphorylation in rat brain mitochondria. Cell Mol Life Sci. 2010.

50. Bandyopadhyay U, Cuervo AM. Chaperone-mediated autophagy in aging and neurodegeneration: lessons from alpha-synuclein. Experimental gerontology. 2007;42(1-2):120-8.

51. Lee HJ, Khoshaghideh F, Patel S, Lee SJ. Clearance of alpha-synuclein oligomeric intermediates via the lysosomal degradation pathway. The Journal of neuroscience : the official journal of the Society for Neuroscience. 2004;24(8):1888-96.

52. Li W, West N, Colla E, Pletnikova O, Troncoso JC, Marsh L, et al. Aggregation promoting C-terminal truncation of alpha-synuclein is a normal cellular process and is enhanced by the familial Parkinson's disease-linked mutations. Proceedings of the National Academy of Sciences of the United States of America. 2005;102(6):2162-7.

53. Okochi M, Walter J, Koyama A, Nakajo S, Baba M, Iwatsubo T, et al. Constitutive phosphorylation of the Parkinson's disease associated alpha-synuclein. The Journal of biological chemistry. 2000;275(1):390-7.

54. Pronin AN, Morris AJ, Surguchov A, Benovic JL. Synucleins are a novel class of substrates for G protein-coupled receptor kinases. The Journal of biological chemistry. 2000;275(34):26515-22.

55. Fujiwara H, Hasegawa M, Dohmae N, Kawashima A, Masliah E, Goldberg MS, et al. alpha-Synuclein is phosphorylated in synucleinopathy lesions.

Nature cell biology. 2002;4(2):160-4.

56. Savitt JM, Dawson VL, Dawson TM. Diagnosis and treatment of Parkinson disease: molecules to medicine. The Journal of clinical investigation. 2006;116(7):1744-54.

57. Arregui CO, Balsamo J, Lilien J. Impaired integrin-mediated adhesion and signaling in fibroblasts expressing a dominant-negative mutant PTP1B. The Journal of cell biology. 1998;143(3):861-73.

58. Cheng A, Bal GS, Kennedy BP, Tremblay ML. Attenuation of adhesion-dependent signaling and cell spreading in transformed fibroblasts lacking protein tyrosine phosphatase-1B. The Journal of biological chemistry. 2001;276(28):25848-55.

초 록

파킨슨 병의 주요 원인 물질로 알려진 알파 시누클레인은 열에 적응성이 있고, 쉽게 응집되는 특성을 가지고 있으며 유비퀴틴-프로테아좀 경로와 샤페론-라이소좀 경로를 통해 분해될 수 있다. 그러나 이 두 경로간의 전환 메커니즘에 대해서는 잘 알려지지 않았다. 본 연구는 프로테아좀의 활성을 저해했을 때 HSC70에 대한 알파 시누클레인의 결합과 알파 시누클레인의 라이소좀으로의 이동이 증가하는 것을 확인하였다. 이 시점에서 알파 시누클레인의 타이로신 136번 잔기의 인산화는 두 분자간의 결합을 증가시킨다. 또한 알파 시누클레인의 타이로신 136번의 인산화가 FAK과 PTP1B에 의해 조절될 수 있다는 것을 확인 하였다. 게다가 PTP1B 저해제는 SH-SY5Y 세포 내에서 알파 시누클레인의 축적을 예방할 수 있었고, 파킨슨 병 모델에서 세포 사멸로부터 도파민성 신경세포를 보호하고, 행동 실험 중 하나인 로타로드 수행 능력을 향상시켰다. 따라서 본 연구결과는 알파 시누클레인의 타이로신 136번 잔기의 인산화 조절이 알파 시누클레인의 라이소좀 분해 경로를 촉진시킴으로써 행동 이상을 개선시킬 수 있으며 세포 사멸로부터 도파민성 신경세포를 보호할 수 있다는 증거를

제시한다.

주요어: 알파 시누클레인, 프로테아좀, 라이소좀, 분해, 파킨슨병, 인산화

학 번: 2006-30572